J. Cell. Mol. Med. Vol 14, No 7, 2010 pp. 1935-1945

Transactin: a universal transmembrane delivery system for *Strep*-tag II-fused cargos

Markus A. Moosmeier [a, *], Julia Bulkescher [a], Jennifer Reed [b], Martina Schnölzer [c], Hans Heid [d], Karin Hoppe-Seyler [a], Felix Hoppe-Seyler [a]

[a] Molecular Therapy of Virus-Associated Cancers, German Cancer Research Center, Heidelberg, Germany
[b] Structural Biochemistry, German Cancer Research Center, Heidelberg, Germany
[c] Functional Proteome Analysis, German Cancer Research Center, Heidelberg, Germany
[d] Helmholtz Group for Cell Biology, German Cancer Research Center, Heidelberg, Germany

Received: March 18, 2009; Accepted: June 29, 2009

Abstract

The delivery of molecules into cells poses a critical problem that has to be solved for the development of diagnostic tools and therapeutic agents acting on intracellular targets. Cargos which by themselves cannot penetrate cellular membranes due to their biophysical properties can achieve cell membrane permeability by fusion to protein transduction domains (PTDs). Here, we engineered a universal delivery system based on PTD-fused *Strep*-Tactin, which we named Transtactin. Biochemical characterization of Transtactin variants bearing different PTDs indicated high thermal stabilities and robust secondary structures. Internalization studies demonstrated that Transtactins facilitated simple and safe transport of *Strep*-tag II-linked small molecules, peptides and multicomponent complexes, or biotinylated proteins into cultured human cells. Transtactin-introduced cargos were functionally active, as shown for horseradish peroxidase serving as a model protein. Our results demonstrate that Transtactin provides a universal and efficient delivery system for *Strep*-tag II-fused cargos.

Keywords: protein transduction • drug delivery • streptavidin • biosafety

Introduction

The delivery of molecules through the plasma membrane into cells is a major technical obstacle for the development of diagnostic tools or therapeutic agents acting on intracellular targets. In many cases, molecules cannot penetrate cellular membranes due to their biophysical properties. This is especially true for peptides and proteins containing polar or even charged side chains.

One way to achieve internalization is the fusion of cargos to ligands of cell-surface receptors. Following receptor–ligand interaction, the cargo is taken up into endosomal compartments by receptor-mediated endocytosis [1, 2]. After endosomal escape, the therapeutic agent, for instance, can inhibit a given target protein by blocking its active site. However, this method requires the covalent coupling of a ligand to the cargo which often leads to altered properties with respect to ligand affinity as well as to the activity of the cargo. Moreover, this targeted approach is highly restricted to certain cell types that express a certain cell-surface receptor and to the internalization properties of the targeted receptor.

An alternative way to induce cell membrane permeability of the cargo is its linkage to protein transduction domains (PTDs), also known as cell penetrating peptides. A PTD is a short peptide comprising an amino acid sequence, which enables it to induce its own internalization into a variety of eukaryotic cell types. Examples of well-studied cationic PTDs are the Tat13 peptide of the HIV-1 *trans*-activator protein (YGRKKRRQRRRPP) [3–7], penetratin, also known as Ant16 (RQIKIWFQNRRMKWKK) [7, 8] and Ant7 (RRMKWKK) [7], both derived from the homeodomain of the *Drosophila melanogaster* Antennapedia protein, or polyarginines like R_9 [7, 9, 10]. Since their discovery in 1988 [3, 4], a broad range of bioactive molecules has been delivered by PTDs into cells both *in vitro* and *in vivo* [11]. This technology is thus considered to bear enormous potential to introduce macromolecular therapeutics into cells [12, 13]. Notably, PTDs can also penetrate intact

*Correspondence to: Markus A. MOOSMEIER,
Molecular Therapy of Virus-Associated Cancers,
German Cancer Research Center,
Im Neuenheimer Feld 242, 69120 Heidelberg, Germany.
Tel.: +49-62 21-42 46 63
Fax: +49-62 21-42 48 52
E-mail: m.moosmeier@dkfz.de

doi:10.1111/j.1582-4934.2009.00846.x

epidermis and dermis, which enables the transdermal delivery of cargos upon topical application [14–16].

However, the genetic fusion of PTDs to cargos can result in reduced protein expression and purification levels [7]. Moreover, the genetic or chemical linkage of PTDs can impair the biophysical properties of the cargo [7]. Therefore, attempts have been made to generate universal cell permeable transporters that allow the concomitant internalization of cargos by non-covalent binding of ligand-fused cargos. Cargos fused to streptavidin (SA), an extracellular homotetrameric protein secreted by the bacterium *Streptomyces avidinii* [17], were delivered into cells by PTD-biotin [18, 19], on the basis of the high affinity of the SA/biotin interaction [20]. *Vice versa*, SA linked to the Tat-PTD was generated as a transporter for biotinylated proteins [21, 22]. However, biotinylation requires chemical linkage and may be inefficient for some cargos, leading to the biotinylation of only a small portion of the cargo. Furthermore, it cannot be excluded that biotinylation of a cargo or its fusion to a scaffold, like SA, may impair its activity. To overcome possible difficulties due to chemical modifications of the cargo, Futaki *et al.* synthesized a cell-permeable nickel-nitrilotriacetic acid (R_8-Ni-NTA) for polyhistidine tagged recombinant proteins [23].

As an alternative for polyhistidine/Ni-NTA, the *Strep*-tag II system has become very common for one-step purification of proteins or high-affinity detection [24]. The *Strep*-tag II peptide (WSHPQFEK) can be easily fused to recombinant proteins during DNA subcloning without the necessity of cross-linking. Moreover, *Strep*-tag II is regarded as biologically inert, proteolytically stable and does usually not interfere with membrane translocation or protein function [24]. Notably, *Strep*-tag II exhibits intrinsic affinity (K_D of 1 μM) towards *Strep*-Tactin (ST), a derivative of SA [25].

Here, we engineered and biochemically characterized a series of PTD-ST transporters which we named Transtactins (derived from transduction and *Strep*-Tactin) (schematic model in Fig. 1). We tested their ability to internalize several model cargos into human cells which included (*i*) FITC-*Strep*-tag II, a cell-impermeable small molecule, (*ii*) His_6-*Strep*-tag II complexed with Ni-NTA-fused horseradish peroxidase (HRP), a proteinaceous multicomponent complex and (*iii*) biotin-HRP, a biotin-linked model compound. Cellular uptake and intracellular distribution of Transtactins and Transtactin-linked cargos were analysed. HRP activities were determined to test whether cargo proteins remain functional upon intracellular delivery by Transtactins.

Materials and methods

Construction, expression and purification of PTD-*Strep*-Tactin

Escherichia coli strain TG2 was used as host for cloning. The pET-21a plasmid (Novagen, Darmstadt, Germany) encoding core SA was kindly provided by P.S. Stayton. ST was expressed from the same vector backbone after QuikChange mutagenesis (Stratagene, Heidelberg, Germany) of the SA portion with primers 5′-G ACC GGT ACC TAC **ATC GGT** GCG **AGG** GGT AAC GCT GAA TC-3′ and 5′-GA TTC AGC GTT ACC **CCT** CGC **ACC GAT** GTA GGT ACC GGT C-3′ (bold letters indicate mutations to induce amino acid substitutions $E^{44}I$, $S^{45}G$ and $V^{47}R$ which convert SA into ST [25]). PTD-ST fusions were generated by PCR-amplification using *Taq* DNA polymerase (Invitrogen, Karlsruhe, Germany), primers 5′-G GAA TTC CAT ATG **CGC CAG ATT AAG ATT TGG TTC CAG AAC CGC CGC ATG AAG TGG AAG AAG** GGT GCT GAA GCT GGT ATC ACC GGC ACC-3′ for Ant16-ST, 5′-G GAA TTC CAT ATG **CGT CGT ATG AAG TGG AAG AAG** GGT GCT GAA GCT GGT ATC ACC GGC ACC-3′ for Ant7-ST, 5′-G GAA TTC CAT ATG **TAC GGA AGA AAG AAG CGC AGA CAA AGA AGA CGT CCA CCA** GGT GCT GAA GCT GGT ATC ACC GGC ACC-3′ for Tat13-ST, 5′-G GAA TTC CAT ATG **AGA CGC AGA AGA AGA AGA AGA CGC AGA** GGT GCT GAA GCT GGT ATC ACC GGC ACC-3′ for R_9-ST (bold letters denote the respective PTD sequences), and reverse primer 5′-CGC AAG CTT TTA TTA GGA AGC AGC GG-3′. PCR-products were digested with *Nde*I and *Hind*III (New England Biolabs, Frankfurt, Germany) and subsequently ligated into linearized pET-21a. All expression vectors were confirmed by DNA sequencing.

SA and (PTD-)ST proteins were expressed in BL21(DE3) (Stratagene) as cytoplasmic insoluble inclusion bodies that were harvested, solubilized, refolded and purified by fractionated ammonium sulphate precipitation [26]. SA and (PTD-)ST proteins were dissolved in PBS buffer and stored at –80°C. Purified proteins were analysed by SDS-PAGE, matrix-assisted laser desorption/ionization (MALDI) time of flight (TOF) mass spectrometry (MS) and circular dichroism (CD) spectroscopy.

Peptide synthesis

FITC-*Strep*-tag II and His_6-*Strep*-tag II peptides were chemically synthesized at the Peptide Synthesis Core Facility of the German Cancer Research Center (Heidelberg, Germany) using Fmoc (N-(9-fluorenyl)methoxycarbonyl) chemistry. Crude peptides were purified by C_{18} reversed phase high-performance liquid chromatography and analysed by MS. Peptide stocks in DMSO (Merck, Darmstadt, Germany) were stored at –80°C and freshly diluted in H_2O.

Cell culture

HeLa, SiHa and U-2 OS cells were cultured in Dulbecco's minimal essential medium (DMEM, Gibco, Eggenstein, Germany), supplemented with 10% foetal bovine serum (FBS, PAA Laboratories, Pasching, Austria), 1% penicillin streptomycin sulphate and 1% of 200 mM L-glutamine (Sigma-Aldrich, Taufkirchen, Germany), at 37°C in 5% CO_2 atmosphere.

Preparation of PTD-ST complexes

(PTD-)ST proteins were complexed with FITC-*Strep*-tag II, biotin-HRP (Pierce, Rockford, IL, USA), or His_6-*Strep*-tag II and Ni-NTA-HRP (Qiagen, Hagen, Germany) by incubation for 15 min. at room temperature. The complexes were directly injected into FBS-free DMEM media of cultured cells.

Edman sequencing

Aliquots of protein samples were spotted on trifluoroacetic acid (TFA)-treated filters (Applied Biosystems, Darmstadt, Germany), dried under

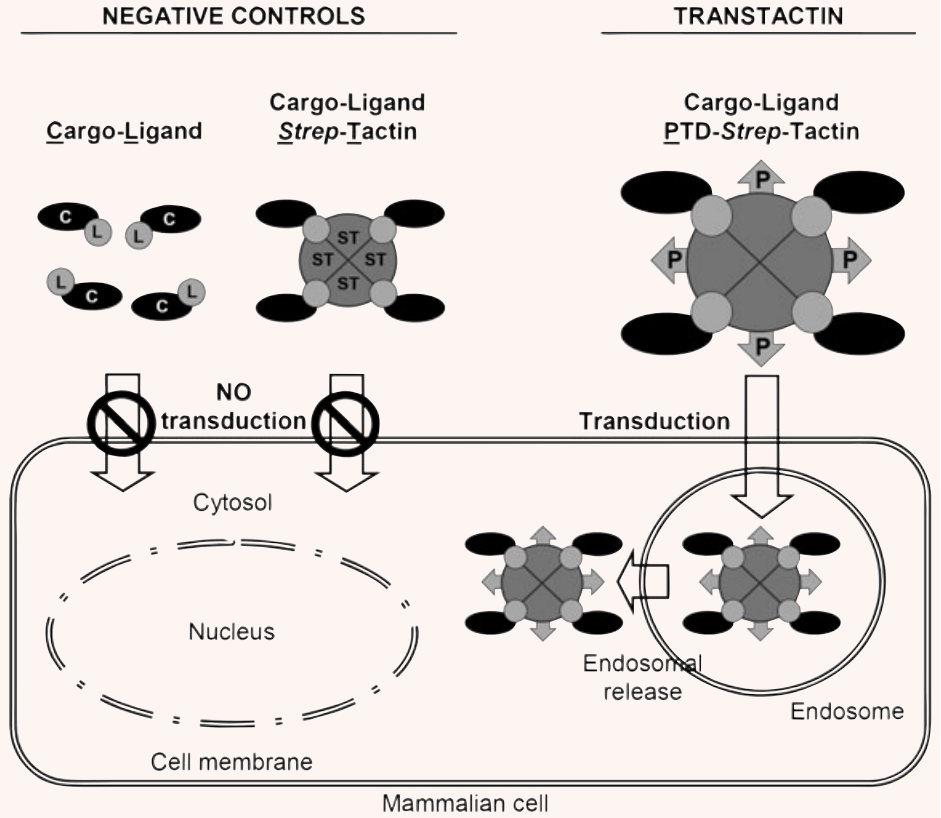

Fig. 1 Transactins. Model for the internalization of a cargo (C) by a PTD (P)-fused ST transporter (termed Transactin). L, ligand, *e.g. Strep*-tag II or biotin. The cargo binds *via* its ligand to Transactin. The PTD portion of Transactin allows subsequent internalization of this complex into mammalian cells, most likely *via* endosomal route (right part of the panel). Ligand-fused cargos *per se*, or ligand-fused cargos bound to ST molecules devoid of a PTD, are not internalized (negative controls, left part of the panel).

nitrogen stream and introduced into a cartridge of an ABI Procise 494 Sequencer (Applied Biosystems) followed by N-terminal Edman sequencing performed with a pulsed-liquid program.

MALDI-TOF mass spectrometry

Prior to MS, protein samples were desalted using C4 ZipTip pipette tips (Millipore, Bedford, MA, USA). Briefly, ZipTips were prewashed with 0.1% TFA (Pierce)/50% acetonitrile (Roth, Karlsruhe, Germany) and equilibrated with 0.1% TFA by repetitive pipetting steps. After loading of the protein samples, ZipTips were washed three times with 0.1% TFA to remove salts. For MALDI-TOF MS 0.3 μl of a saturated solution of sinapinic acid (Bruker-Daltonics, Bremen, Germany) in ethanol were deposited as thin film onto individual spots of a MALDI target plate. Subsequently, proteins were eluted from the ZipTips with 1–2 μl of a saturated solution of sinapinic acid in 0.1% TFA/50% acetonitrile, directly loaded on top of the thin film spots and allowed to co-crystallize slowly at ambient temperature. MALDI mass spectra were recorded in the positive ion linear mode with delayed extraction on a Reflex II TOF instrument (Bruker-Daltonics) equipped with a SCOUT-26 probe and a 337 nm nitrogen laser. Ion acceleration voltage was set to 20.0 kV and the first extraction plate to 17.1 kV. Mass spectra were obtained by averaging up to 200 individual laser shots. Spectra were calibrated externally by a quadratic fit using the singly protonated average masses of ubiquitin I at m/z 8565.89, cytochrom c at m/z 12,361.55 and myoglobin at m/z 16,952.55 (Protein Calibration Standard I, Bruker Daltonics).

Thermal tetramer stability

Three micrograms of purified proteins were combined with SDS-containing sample buffer and heated at selected temperatures for 5 min., then chilled on ice and subsequently analysed by SDS-PAGE. Proteins were stained with Coomassie brilliant blue (Serva, Heidelberg, Germany).

CD spectroscopy

CD spectroscopy was carried out using a J-710 spectropolarimeter (JASCO, Gross-Umstadt, Germany) calibrated with a solution of 0.05% β-androsterone dissolved in dioxane. Sample temperature control during measurement was achieved through use of a JASCO PFD-350S Peltier thermostat. Samples at a concentration of ~100 μg/ml protein in distilled water were scanned in a 1 mm quartz cuvette from 190 to 240 nm for secondary structure determination. Final spectra were the result of four-fold signal averaging. Thermal denaturation spectra were run from 40°C to 95°C at a gradient of 1.0°C/min. Care was taken to ensure that all relevant parameters were identical for the several proteins measured, since properties such as the melting temperature (T_m) are not absolute and vary with measurement conditions. Due to the unusual spectral characteristics of SA and related proteins, the observational wavelength for temperature denaturation was chosen to be 215 nm rather than the standard 222 nm. Secondary structure content was calculated from the far UV CD spectra after subtracting an identically scanned and signal-averaged solvent baseline.

After their conversion to mean residue ellipticity (θ_{mrw}) and removal of residual noise through a fast Fourier transform program, the program PEP-FIT [27] (specifically designed for the secondary structure analysis of peptides rather than globular proteins) was employed for fitting of the processed spectra. The relative T_m of SA and its derivatives was obtained from the denaturation curves using the JASCO Denatured Protein software.

Western blotting

Three micrograms of protein extracts were combined with SDS-containing sample buffer and boiled at 95°C for 5 min., separated by 15% SDS-PAGE, transferred in a semi-dry blotter system (cti, Idstein, Germany) to an Immobilon-P membrane (Millipore) and analysed by enhanced chemiluminescence (GE Healthcare, Munich, Germany). The following antibodies were used: rabbit anti-SA antibody (Sigma-Aldrich, 1:2000), mouse anti-tubulin antibody CP06 (Calbiochem, Schwalbach, Germany, 1:5000) and antimouse and anti-rabbit HRP-labelled secondary antibodies (Promega, Mannheim, Germany, 1:3000).

Fluorescence microscopy

HeLa cells were plated on 35 mm dishes (Greiner Bio-one, Frickenhausen, Germany) at 40% to 60% confluency. 10 μM of (PTD-)ST proteins were complexed with 10 μM FITC-*Strep*-tag II and directly injected into FBS-free media. After a 120-min. incubation at 37°C, 5% CO_2, the cells were washed, trypsinized, plated on glass cover-slips and fixed with 4% paraformaldehyde (Merck) after 4 hrs. Cover slips were stored at –20°C in 70% ethanol. ST was detected using a rabbit anti-SA antibody (1:500) and an anti-rabbit Cy3-labeled secondary antibody (Dianova, Hamburg, Germany, 1:400). Endosomes were visualized with the fluid-phase marker TRITC-dextran (Invitrogen), as described [22]. Cy3-, FITC- and TRITC-signals were detected using a Vanox-T fluorescence microscope (Olympus, Hamburg, Germany) and an F-View camera (Olympus).

HRP assay

HeLa cells were plated on 35 mm dishes at 80% to 90% confluency and treated with 1 μM (PTD-)ST complexed with 1.5 μM His_6-*Strep*-tag II and 2 μM Ni-NTA-HRP or with 2 μM biotin-HRP. Cells were incubated at 37°C, 5% CO_2 for 2 hrs, then trypsinized, washed with 1× PBS and lysed with 400 μl 1× reporter lysis buffer (RLB, Promega). Cell lysates were incubated at room temperature for 15 min. After vortexing and pelleting, the supernatants were stored at –80°C. Extracts were diluted and 40 μl thereof were mixed with 10 μl 1× RLB. At the same time, and under identical conditions, calibration curves were generated using a series of dilutions of ST complexed with His_6-*Strep*-tag II and Ni-NTA-HRP, or biotin-HRP. Complexes were diluted and 10 μl thereof were supplemented with 40 μl of dilutions of untreated HeLa lysates. Colorimetric reactions were initiated by adding 50 μl of 1-Step Ultra TMB-ELISA substrate solution (Pierce). The reaction was stopped by adding 50 μl of 2 M sulphuric acid (Merck) and the absorbance was measured at 450 nm. Calibration curves were fitted using the four parameter logistic (4PL) equation in SigmaPlot 10.0 (Systat Software, Erkrath, Germany). The absorbance was recalculated to the amount of internalized HRP and normalized to the amount of total protein determined by Bradford protein assay as described [28].

Results

Production, purification and characterization of PTD-ST fusion proteins

For generating different Transtactin variants, Ant16, Ant7, Tat13 and R_9 PTDs were fused in frame to the 5′ end of the ST coding sequence and subcloned into pET-21a. Individual Transtactins, as well as unfused SA and ST, were expressed as cytosolic inclusion bodies in *E. coli*. SDS-PAGE analyses of bacterial whole cell extracts indicated that all recombinant proteins were expressed in full length (data not shown). Apart from Ant16-ST which remained denatured, all proteins could be refolded and purified in high yields of over 20 mg/l expression volume by fractionated ammonium sulphate precipitation (data not shown). Proteins were >95% pure as determined by SDS-PAGE analysis (Coomassie-staining, data not shown).

MALDI-TOF MS analyses of purified proteins detected molecular weights as expected for their theoretical masses (MH^+, Table 1). All PTD-ST fusion proteins started with a methionine. In the case of unfused SA or ST, the N-terminal methionines were removed (Table 1), as verified by MALDI-TOF MS analysis and Edman sequencing (data not shown), most likely due to the activity of *E. coli* methionine aminopeptidase [29].

Thermal tetramer stability

SA and ST tetramerization [25] is required for building the binding pocket for biotin and *Strep*-tag II [30]. Both SA and ST tetramers are extremely stable, even in the presence of SDS, and therefore can be detected on SDS-PAGE [31, 32]. Since instability of transporters can restrict their use, the influence of different PTD fusions on the temperature-dependent ST tetramer breakup was studied, as exemplified for Tat13-ST in Fig. 2(A). Up to a temperature of 60°C, all proteins were detectable in a tetrameric state (Fig. 2B). Unfused ST exhibited a slightly reduced tetrameric stability when compared to unfused SA (60°C *versus* 65°C). Notably, all PTD fusions slightly increased the tetramer stability of ST: Ant7-ST showed a tetramer stability of 65°C, Tat13-ST and R_9-ST tetramers were stable up to 70°C (Fig. 2B). At further increased temperatures, the amount of tetramers started to decrease for all proteins, with concomitant appearance of monomeric forms (Fig. 2).

Secondary structure analysis

Since PTD fusions can influence the biophysical properties of cargos [7], far UV CD spectroscopy was performed to assess possible alterations in the secondary structure of ST due to the N-terminal PTD-fusions. The spectra of all Transtactins showed an almost identical curve progression as unfused ST (Fig. 3A), similar to the CD spectrum of SA. CD spectra were interpreted using

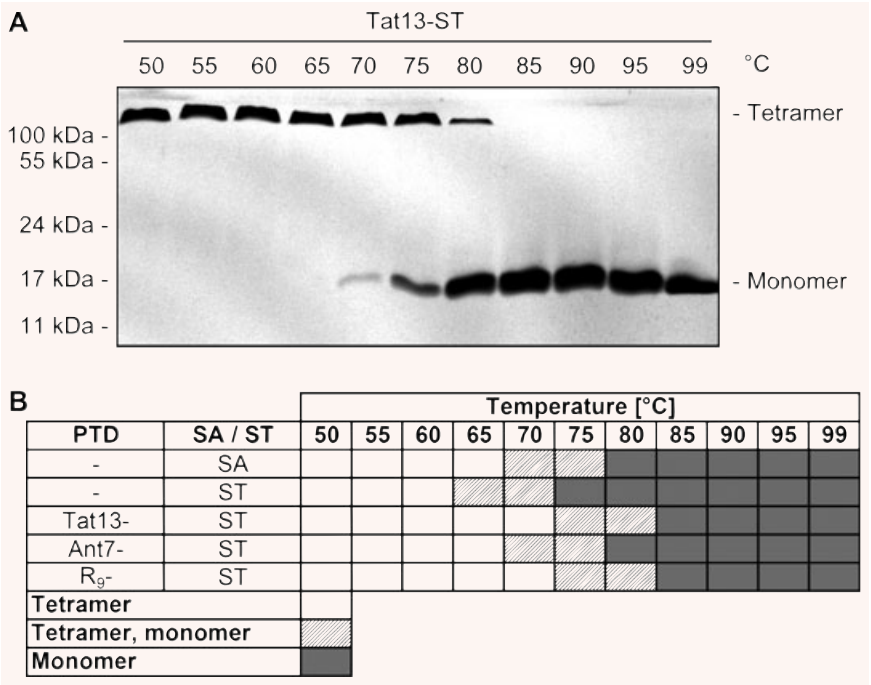

Fig. 2 Thermal tetramer stability of Transtactins. (**A**) SDS-PAGE analysis of Coomassie-stained Tat13-ST at various temperatures. Tetrameric and monomeric states are indicated. (**B**) Compilation of tetramer stabilities of unfused SA or ST, Tat13-ST, Ant7-ST and R_9-ST.

Table 1 Biophysical characterization of Transtactin proteins

Protein	PTD	MALDI-TOF MS		Start-methionine	Melting temperature [°C]
		Calculated MH^+ (av)	Observed MH^+		
SA		13,272.5*	13,273.8	−	83.67 ± 0.34
ST		13,283.6*	13,287.5	−	79.21 ± 0.76
Tat13-ST	YGRKKRRQRRRPP	15,207.9	15,207.1	+	76.46 ± 0.37
Ant7-ST	RRMKWKK	14,486.2	14,485.4	+	75.45 ± 1.22
R_9-ST	RRRRRRRRR	14,877.5	14,882.4	+	74.63 ± 1.51

Mass spectrometry: (*) MH^+ (av): average m/z value calculated without start-methionine. Start-methionine present (+), absent (−). Average melting temperatures were calculated by at least two independently performed thermal unfolding experiments, using CD spectroscopy.

PEPFIT [27]. The fractions of secondary structure were compared with the crystal structures of SA [33] and ST [34] (Fig. 3B). Both the line shapes of the CD spectra and the PEPFIT data indicated that all proteins share similar β-sheet content of approximately 44.5% to 54% and α-helix rates up to 7% (Fig. 3B). These minor differences can be explained by the N-terminal PTD-fusions or slight skewing of the analyses of CD spectra due to the need to compensate for the unusual pronounced positive peaks at 230 nm [35] (most likely one lobe of an exciton interaction between aromatic side chains [36, 37]). Thermal unfolding analyses also revealed that the conformational stabilities of individual Transtactins were comparable, exhibiting high melting temperatures (T_ms) which ranged from 74.63°C for R_9-ST to 76.46°C for Tat13-ST (Table 1).

Internalization of PTD-ST

To investigate the ability of Transtactin proteins to internalize into mammalian cells, HeLa cells were incubated with different

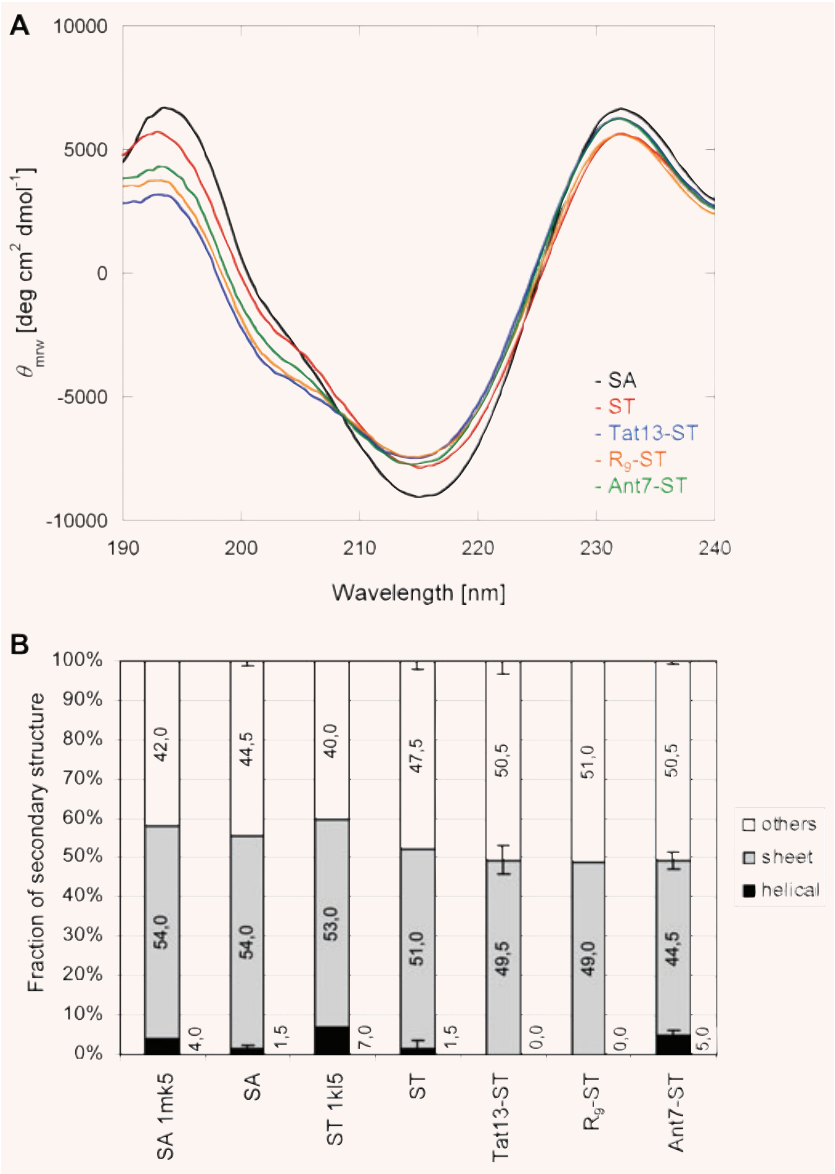

Fig. 3 Secondary structure analyses of Transtactins. (**A**) Far UV CD spectroscopy. (**B**) Interpretation of CD spectra by PEPFIT analysis. Fractions of secondary structure were compared with the crystal structures of SA (PDB entry 1mk5) and ST (PDB entry 1kl5).

concentrations of Tat13-ST for 2 hrs. Titration experiments revealed that internalized Transtactins could be detected by immunoblotting upon external application of doses as low as 100 nM (data not shown). In order to test whether PTD-mediated internalization is cell-type restricted, cultured HeLa and SiHa cervical carcinoma as well as U-2 OS osteosarcoma cells were incubated for 2 hrs with 1 μM of different Transtactin variants or unfused ST. Subsequently, whole cell protein extracts were prepared and analysed by immunoblotting. In contrast to unfused ST, all Transtactins were internalized at readily detectable levels. Tat13-ST and R9-ST reproducibly exhibited a more efficient internalization than Ant7-ST, under identical experimental conditions (Fig. 4).

Intracellular distribution of internalized Transtactins

Next, we analysed the intracellular distribution of internalized Transtactins. HeLa cells were treated with 10 μM of Tat13-ST or R9-ST for 2 hrs. Tat13-ST and R9-ST proteins were detected in almost 100% of the cells (data not shown), either in a punctuated pattern around the cell nucleus or cytosolically solubilized with nuclear exclusion (Fig. 5A). This pattern is consistent with previous reports investigating internalization of PTD-fused cargos which accumulated in the cytosol and in distinct perinuclear inclusions which were subsequently identified as endosomal compartments [21, 22].

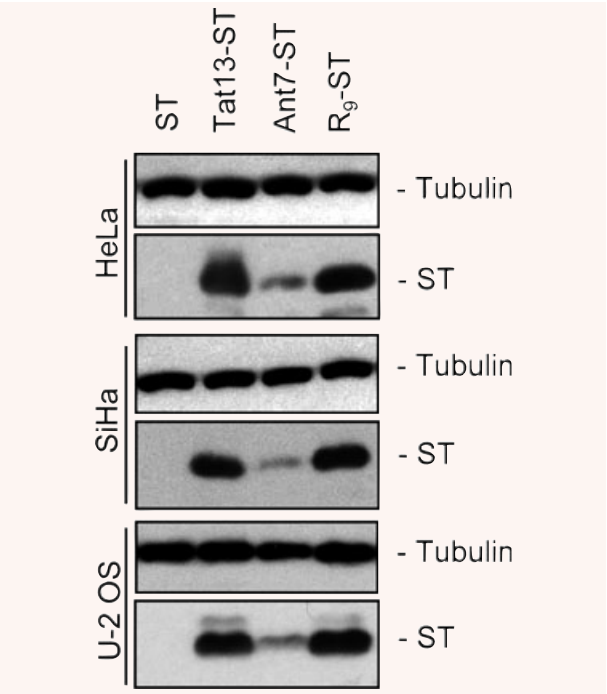

Fig. 4 Internalization of Transtactins into HeLa, SiHa and U-2 OS cells. Immunoblot analyses of whole cell extracts following treatment with Tat13-ST, Ant7-ST and R_9-ST. ST, unfused ST. Tubulin, loading control.

Transtactin-mediated co-internalization of FITC-*Strep*-tag II

In order to investigate whether Transtactins were able to co-internalize a small model molecule linked to *Strep*-tag II, HeLa cells were treated for 2 hrs with Tat13-ST or R_9-ST complexed with FITC-*Strep*-tag II. We observed that FITC-*Strep*-tag II was clearly internalized by both Transtactins (Fig. 5B). In contrast, cells control-treated with FITC-*Strep*-tag II alone or FITC-*Strep*-tag II complexed with unfused ST exhibited only background FITC fluorescent signals (Fig. 5B). Staining pattern for FITC-*Strep*-tag II inside cells was punctual, indicating enrichment in distinct cellular compartments. These signals co-stained with the fluid-phase endosomal marker TRITC-dextran [22] (Fig. 5B), indicating that FITC-*Strep*-tag II is enriched in endosomal compartments, consistent with previous findings for PTD-linked cargos [22, 38].

Internalization of peptides, proteins and complexes by Transtactins

Next, we tested whether Transtactins were also able to deliver *Strep*-tag II-fused peptides, proteins and multicomponent complexes into cells. To this end, Tat13-ST or R_9-ST Transtactins were complexed with His_6-*Strep*-tag II and Ni-NTA-HRP. In this scenario, the Ni-NTA-HRP portion should be non-covalently linked to the Transtactins *via* His_6-*Strep*-tag II. Two hours following treatment of HeLa cells with these three-component complexes, high enzymatic HRP activities were measured in cellular lysates (Fig. 6A). Cells incubated with Ni-NTA-HRP alone (data not shown), or with a three-component complex of unfused ST, His_6-*Strep*-tag II and Ni-NTA-HRP (Fig. 6A), showed only background enzymatic HRP activities.

The capacity of Transtactins to internalize proteins in a functional form was further confirmed by using biotin-HRP as a cargo under identical experimental conditions as described for the internalization of Ni-NTA-HRP. Again, high enzymatic HRP activities were measured in HeLa cells treated with complexes of Tat13-ST or R_9-ST, and biotin-HRP (Fig. 6A). In contrast, cells incubated with biotin-HRP alone (data not shown) or with a complex of unfused ST with biotin-HRP (Fig. 6A) showed only background HRP activities. The concentrations of internalized HRP ranged from 8 to 15 pmol/mg (Fig. 6B).

Discussion

Cell permeable ST derivatives, termed Transtactins, were developed as a universal internalization system for *Strep*-tag II- or biotin-linked compounds. Cargos successfully internalized included FITC-*Strep*-tag II as a model compound for a small cell-impermeable cargo, His_6-*Strep*-tag II complexed with Ni-NTA-HRP as a model for a multicomponent proteinaceous complex, and biotin-HRP as a model biotinylated cargo. The introduction of *Strep*-tag II-fused cargos revealed that a K_D of 1 μM is sufficient for Transtactin-mediated internalization. Transtactin-introduced HRPs were enzymatically active, showing that the system allows the internalization of functionally active proteins.

Transtactin proteins were produced as insoluble inclusion bodies in *E. coli*. Apart from Ant16-ST which remained denatured and could not be refolded, all proteins could be purified by fractionated ammonium sulphate precipitation [26]. The expression of Transtactins as inclusion bodies thus seems to prevent the common problems of both reduced expression levels and purification yields for PTD-fused cargos [7] since high amounts of over 20 mg/l purified proteins for the Transtactins were obtained.

The fusion of Tat13, Ant7 and R_9 to ST only slightly altered its secondary structure, indicating that ST is an extremely rigid protein scaffold. This is an important requirement to retain the *Strep*-tag II-binding property of ST, following PTD fusion. SA and ST tetramerization [25] is essential to correctly form the biotin- and *Strep*-tag II-binding pocket which lies in the interface between SA and ST subunits [30]. High thermal tetramer stabilities were measured for all engineered Transtactin variants, as reported for SA [31, 32], indicating that Transtactins are stable within a wide temperature range and that no cooling at the bench or during storage and shipping is required.

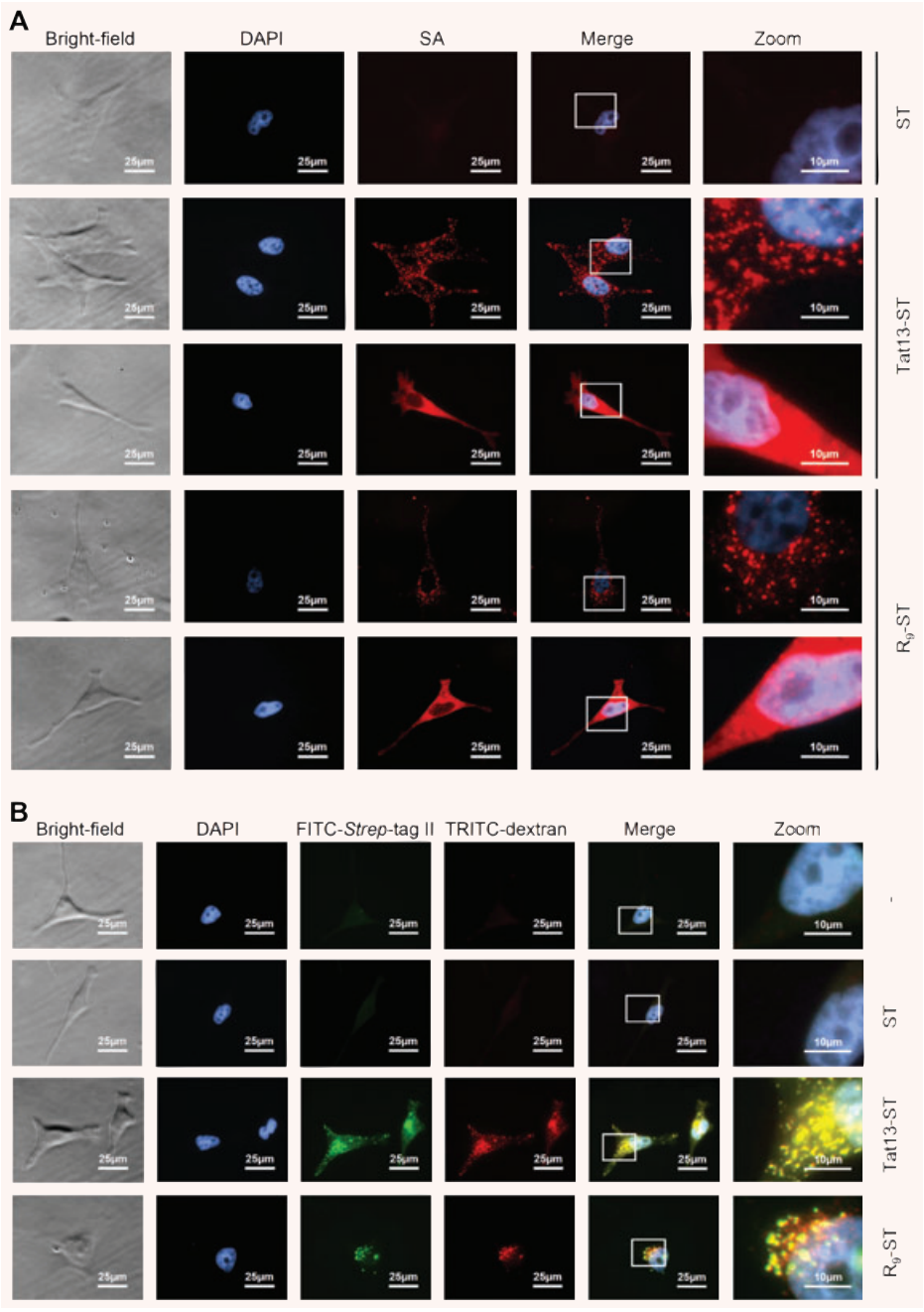

Fig. 5 (**A**) Intracellular distribution of Transtactin proteins. Fluorescence microscopy of HeLa cells treated with unfused ST, Tat13-ST and R_9-ST. Transtactins exhibited either a punctuated pattern around the nucleus (upper panels for Tat13-ST and R_9-ST) or diffuse cytosolic staining (lower panels for Tat13-ST and R_9-ST). Zoom, higher resolution of the boxed areas. Treatment of SiHa or U-2 OS cells yielded identical results (data not shown). (**B**) Intracellular distribution of FITC-*Strep*-tag II internalized by Transtactins. Fluorescence microscopy of HeLa cells treated with FITC-*Strep*-tag II alone, FITC-*Strep*-tag II complexed with unfused ST, FITC-*Strep*-tag II complexed with Tat13-ST and FITC-*Strep*-tag II complexed with R_9-ST. TRITC-dextran, fluid-phase endosomal marker.

All Transtactins were able to efficiently induce their own internalization into human cell lines derived from epithelial (HeLa, SiHa) or connective tissues (U-2 OS), in line with reports showing that PTD-linked compounds penetrate into a wide range of cell types [11]. Titration experiments revealed that internalization of Transtactins could be detected upon external application of doses as low as 100 nM. The precise uptake mechanism of PTD-linked cargos is currently a topic of lively discussion. However, in the case of cationic PTDs, it is most likely that the positively charged side chains interact with the anionic structure at the cell surface leading to an increased local concentration of PTDs, subsequently allowing cellular entry by a fluid-phase endocytotic mechanism *via* endosomal compartments [38]. Consistent with this proposed mechanism, Transtactins were found either diffusively distributed

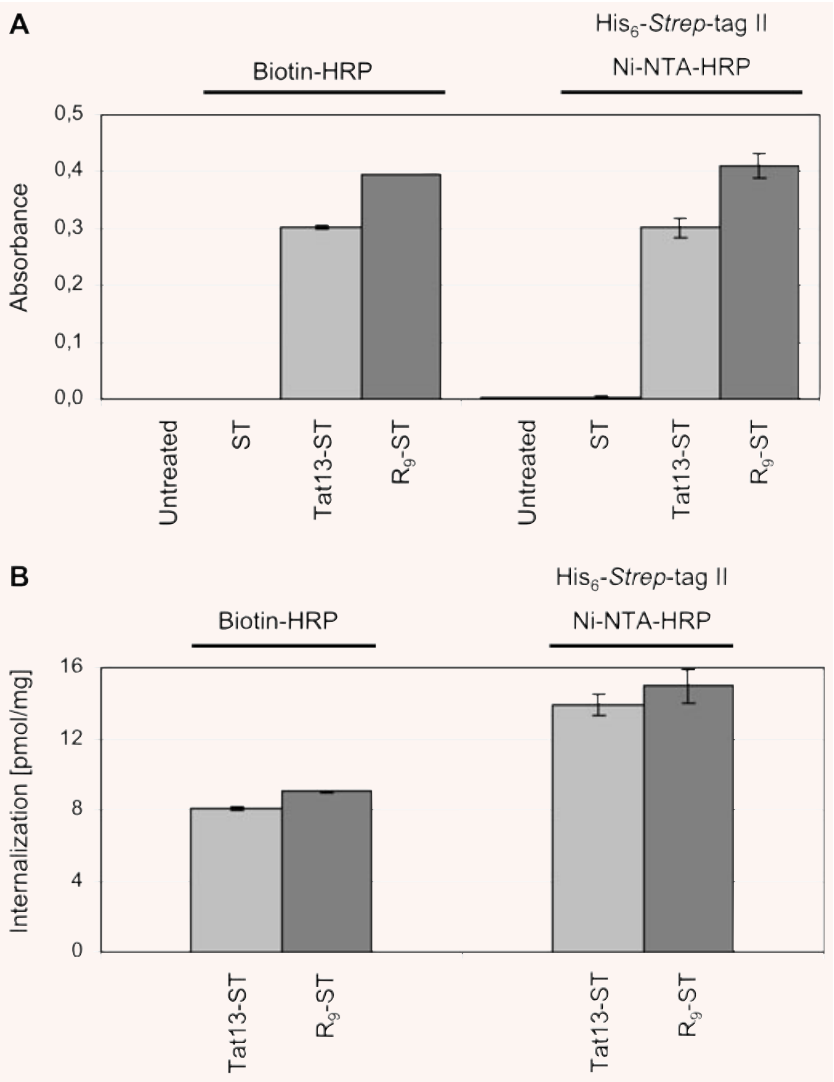

Fig. 6 Internalization of functional HRP by Tat13-ST and R_9-ST. (**A**) Analysis of enzymatic HRP activities upon internalization of His_6-*Strep*-tag II complexed with Ni-NTA-HRP or biotin-HRP, by the indicated Transactins. Cells treated with either ST alone, or Ni-NTA-HRP complexed with His_6-*Strep*-tag II, or biotin-HRP, showed no HRP activities (data not shown). (**B**) Absorbance was recalculated to the amount of both internalized HRP and total protein. Uptake results are expressed as pmol of HPR per mg of total protein.

in the cytoplasm or in endosomal compartments as previously shown for Tat-SA [21, 22]. Notably, Transactins were even able to internalize a proteinaceous complex including Ni-NTA-HPR or biotinylated HRP with a total MW of ~220 kD. The internalization efficiencies of HPR ranged between 8 and 15 pmol/mg total protein which is within the same range as reported for Tat-biotin-internalized FITC-SA (~23 pmol/mg) [28] with a total MW of only ~60 kD. As previously reported [9, 10], we found that internalization efficiencies increased with rising numbers of positively charged residues within the PTD portion (Ant7 < Tat13 < R_9) of the different Transactin variants.

The application of Transactins is straightforward. Only a short incubation step of the transporter with the cargo in buffer conditions is necessary for complex formation. Then, the complex is injected into serum- and biotin-free medium of cultured cells. Free biotin in the cell culture medium can be removed with avidin, a biotin-binding protein that does not interfere with *Strep*-tag II [24]. No further treatment or expensive laboratory equipment is required for internalization.

Transactin transporters possess several advantages over the existing cargo delivering system Tat-SA [21, 22]. Firstly, the *Strep*-tag II/ST system has become very common for purification of various cargos. *Strep*-tag II can be easily fused to the N- or C-terminus of any kind of recombinant protein during subcloning [24] using *Strep*-tag II-expression vectors which are available for various host organisms [24]. Thus, no elaborate chemical linkage, as in the case of biotin, is necessary. Secondly, biotinylation often requires spacer arms between biotin and the cargo to reduce steric hindrance which can interfere with binding to SA. Typical spacers, such as a 6 carbon spacer [39], often reduce the solubility

of the cargo in aqueous media which is problematic for *in vivo* applications where organic solvents cannot be used. In contrast to biotin, *Strep*-tag II requires, if at all, only a short two amino acid spacer to ensure accessibility [24]. Thirdly, unlike *Strep*-tag II [24], biotinylation may disturb cargo functions due to the chemical linkage.

Transtactins also should have advantages over the introduction of cargos which are directly linked to a PTD. Firstly, PTD-fused cargos often suffer from reduced expression and purification levels [7] in contrast to *Strep*-tag II-cargos prepared for internalization by Transtactins. Secondly, PTD-fused agents have been shown to penetrate intact skin [14–16] indicating that they could pose a health risk for experimentators working with potentially hazardous compounds. The fact that Transtactins and the cargo can be produced separately increases the bio-safety during preparation since ST has no reported biological functions apart from biotin-binding properties and the cargo cannot penetrate into cells without the transporter. Thirdly, by employing suitable linkers, the internalization of alternatively tagged cargos is also conceivable, *e.g.* using biotin-Ni-NTA linkers [40–42] for His_6-fused proteins.

In summary, Transtactins meet the requirements for universal delivery systems for *Strep*-tag II-fused cargos. They thus fill the remaining gap between unspecific traditional transfection methods, like lipofection and cell-surface receptor-mediated endocytosis of ligand-fused cargos. Possible applications of Transtactins range from basic proteomics research to high-throughput testing of intracellularly active diagnostics [7, 43] and non-cell permeable therapeutic peptides [44, 45] and proteins [46–48]. Moreover, it could be envisioned to develop Transtactins as transporters for therapeutically useful cargos in human beings. However, at present, this latter issue still faces technical hurdles associated with protein therapeutics in general which include proteolytic instability of PTDs [49] and antigenicity of SA [50]. Possible solutions to reduce the potential antigenicity of Transtactins include site-directed mutagenesis of solvent-exposed side chains, as shown for SA [51], or replacement of ST by non-immunogenic scaffolds, like human-derived lipocalins [52, 53], engineered to bind protein tags, such as *Strep*-tag II or His_6.

Acknowledgements

The authors are grateful to P.S. Stayton (University of Washington, WA, USA) for the core SA expression vector, A. Hunziker (Sequencing Core Facility, German Cancer Research Center) for DNA-sequencing and R. Pipkorn (Peptide Synthesis Core Facility, German Cancer Research Center) for peptide synthesis.

References

1. **Qian ZM, Li H, Sun H *et al.*** Targeted drug delivery via the transferrin receptor-mediated endocytosis pathway. *Pharmacol Rev.* 2002; 54: 561–87.
2. **Wileman T, Harding C, Stahl P.** Receptor-mediated endocytosis. *Biochem J.* 1985; 232: 1–14.
3. **Frankel AD, Pabo CO.** Cellular uptake of the tat protein from human immunodeficiency virus. *Cell.* 1988; 55: 1189–93.
4. **Green M, Loewenstein PM.** Autonomous functional domains of chemically synthesized human immunodeficiency virus tat trans-activator protein. *Cell.* 1988; 55: 1179–88.
5. **Fawell S, Seery J, Daikh Y *et al.*** Tat-mediated delivery of heterologous proteins into cells. *Proc Natl Acad Sci USA.* 1994; 91: 664–8.
6. **Vives E, Brodin P, Lebleu B.** A truncated HIV-1 Tat protein basic domain rapidly translocates through the plasma membrane and accumulates in the cell nucleus. *J Biol Chem.* 1997; 272: 16010–7.
7. **Honda A, Moosmeier MA, Dostmann WR.** Membrane-permeable cygnets: rapid cellular internalization of fluorescent cGMP-indicators. *Front Biosci.* 2005; 10: 1290–301.
8. **Derossi D, Joliot AH, Chassaing G *et al.*** The third helix of the Antennapedia homeodomain translocates through biological membranes. *J Biol Chem.* 1994; 269: 10444–50.
9. **Mitchell DJ, Kim DT, Steinman L *et al.*** Polyarginine enters cells more efficiently than other polycationic homopolymers. *J Pept Res.* 2000; 56: 318–25.
10. **Futaki S, Suzuki T, Ohashi W *et al.*** Arginine-rich peptides. An abundant source of membrane-permeable peptides having potential as carriers for intracellular protein delivery. *J Biol Chem.* 2001; 276: 5836–40.
11. **Dietz GP, Bahr M.** Delivery of bioactive molecules into the cell: the Trojan horse approach. *Mol Cell Neurosci.* 2004; 27: 85–131.
12. **Gump JM, Dowdy SF.** TAT transduction: the molecular mechanism and therapeutic prospects. *Trends Mol Med.* 2007; 13: 443–8.
13. **Trehin R, Merkle HP.** Chances and pitfalls of cell penetrating peptides for cellular drug delivery. *Eur J Pharm Biopharm.* 2004; 58: 209–23.
14. **Park J, Ryu J, Jin LH *et al.*** 9-polylysine protein transduction domain: enhanced penetration efficiency of superoxide dismutase into mammalian cells and skin. *Mol Cells.* 2002; 13: 202–8.
15. **Jin LH, Bahn JH, Eum WS *et al.*** Transduction of human catalase mediated by an HIV-1 TAT protein basic domain and arginine-rich peptides into mammalian cells. *Free Radic Biol Med.* 2001; 31: 1509–19.
16. **Rothbard JB, Garlington S, Lin Q *et al.*** Conjugation of arginine oligomers to cyclosporin A facilitates topical delivery and inhibition of inflammation. *Nat Med.* 2000; 6: 1253–7.
17. **Green NM.** Avidin and streptavidin. *Methods Enzymol.* 1990; 184: 51–67.
18. **Mi Z, Mai J, Lu X *et al.*** Characterization of a class of cationic peptides able to facilitate efficient protein transduction in vitro and in vivo. *Mol Ther.* 2000; 2: 339–47.
19. **Mai JC, Shen H, Watkins SC *et al.*** Efficiency of protein transduction is cell type-dependent and is enhanced by dextran sulfate. *J Biol Chem.* 2002; 277: 30208–18.
20. **Laitinen OH, Nordlund HR, Hytonen VP *et al.*** Brave new (strept)avidins in biotechnology. *Trends Biotechnol.* 2007; 25: 269–77.

21. **Albarran B, To R, Stayton PS.** A TAT-streptavidin fusion protein directs uptake of biotinylated cargo into mammalian cells. *Protein Eng Des Sel.* 2005; 18: 147–52.
22. **Rinne J, Albarran B, Jylhava J *et al.*** Internalization of novel non-viral vector TAT-streptavidin into human cells. *BMC Biotechnol.* 2007; 7: 1.
23. **Futaki S, Niwa M, Nakase I *et al.*** Arginine carrier peptide bearing Ni(II) chelator to promote cellular uptake of histidine-tagged proteins. *Bioconjug Chem.* 2004; 15: 475–81.
24. **Schmidt TG, Skerra A.** The Strep-tag system for one-step purification and high-affinity detection or capturing of proteins. *Nat Protoc.* 2007; 2: 1528–35.
25. **Voss S, Skerra A.** Mutagenesis of a flexible loop in streptavidin leads to higher affinity for the Strep-tag II peptide and improved performance in recombinant protein purification. *Protein Eng.* 1997; 10: 975–82.
26. **Schmidt TG, Skerra A.** One-step affinity purification of bacterially produced proteins by means of the "Strep tag" and immobilized recombinant core streptavidin. *J Chromatogr A.* 1994; 676: 337–45.
27. **Reed J, Reed TA.** A set of constructed type spectra for the practical estimation of peptide secondary structure from circular dichroism. *Anal Biochem.* 1997; 254: 36–40.
28. **El-Andaloussi S, Jarver P, Johansson HJ *et al.*** Cargo dependent cytotoxicity and delivery efficacy of cell-penetrating peptides: a comparative study. *Biochem J.* 2007; 407: 285–92.
29. **Mogk A, Schmidt R, Bukau B.** The N-end rule pathway for regulated proteolysis: prokaryotic and eukaryotic strategies. *Trends Cell Biol.* 2007; 17: 165–72.
30. **Sano T, Cantor CR.** Intersubunit contacts made by tryptophan 120 with biotin are essential for both strong biotin binding and biotin-induced tighter subunit association of streptavidin. *Proc Natl Acad Sci USA.* 1995; 92: 3180–4.
31. **Waner MJ, Navrotskaya I, Bain A *et al.*** Thermal and sodium dodecylsulfate induced transitions of streptavidin. *Biophys J.* 2004; 87: 2701–13.
32. **Bayer EA, Ehrlich-Rogozinski S, Wilchek M.** Sodium dodecyl sulfate-polyacrylamide gel electrophoretic method for assessing the quaternary state and comparative thermostability of avidin and streptavidin. *Electrophoresis.* 1996; 17: 1319–24.
33. **Hyre DE, Le Trong I, Merritt EA *et al.*** Cooperative hydrogen bond interactions in the streptavidin-biotin system. *Protein Sci.* 2006; 15: 459–67.
34. **Korndorfer IP, Skerra A.** Improved affinity of engineered streptavidin for the Strep-tag II peptide is due to a fixed open conformation of the lid-like loop at the binding site. *Protein Sci.* 2002; 11: 883–93.
35. **Green NM, Melamed MD.** Optical rotatory dispersion, circular dichroism and far-ultraviolet spectra of avidin and streptavidin. *Biochem J.* 1966; 100: 614–21.
36. **Grishina IB, Woody RW.** Contributions of tryptophan side chains to the circular dichroism of globular proteins: exciton couplets and coupled oscillators. *Faraday discussions.* 1994: 245–62.
37. **Mandal K, Bose SK, Chakrabarti B *et al.*** Structure and stability of gamma-crystallins. I. Spectroscopic evaluation of secondary and tertiary structure in solution. *Biochim Biophys Acta.* 1985; 832: 156–64.
38. **Brooks H, Lebleu B, Vives E.** Tat peptide-mediated cellular delivery: back to basics. *Adv Drug Deliv Rev.* 2005; 57: 559–77.
39. **Hnatowich DJ, Virzi F, Rusckowski M.** Investigations of avidin and biotin for imaging applications. *J Nucl Med.* 1987; 28: 1294–302.
40. **McMahan SA, Burgess RR.** Single-step synthesis and characterization of biotinylated nitrilotriacetic acid, a unique reagent for the detection of histidine-tagged proteins immobilized on nitrocellulose. *Anal Biochem.* 1996; 236: 101–6.
41. **O'Shannessy DJ, O'Donnell KC, Martin J *et al.*** Detection and quantitation of hexahistidine-tagged recombinant proteins on western blots and by a surface plasmon resonance biosensor technique. *Anal Biochem.* 1995; 229: 119–24.
42. **Reichel A, Schaible D, Al Furoukh N *et al.*** Noncovalent, site-specific biotinylation of histidine-tagged proteins. *Anal Chem.* 2007; 79: 8590–600.
43. **Sawyer CL, Honda A, Dostmann WR.** Cygnets: spatial and temporal analysis of intracellular cGMP. *Proc West Pharmacol Soc.* 2003; 46: 28–31.
44. **Borghouts C, Kunz C, Groner B.** Current strategies for the development of peptide-based anti-cancer therapeutics. *J Pept Sci.* 2005; 11: 713–26.
45. **Prive GG, Melnick A.** Specific peptides for the therapeutic targeting of oncogenes. *Curr Opin Genet Dev.* 2006; 16: 71–7.
46. **Borghouts C, Kunz C, Delis N *et al.*** Monomeric recombinant peptide aptamers are required for efficient intracellular uptake and target inhibition. *Mol Cancer Res.* 2008; 6: 267–81.
47. **Colas P.** Combinatorial protein reagents to manipulate protein function. *Curr Opin Chem Biol.* 2000; 4: 54–9.
48. **Hoppe-Seyler F, Crnkovic-Mertens I, Tomai E *et al.*** Peptide aptamers: specific inhibitors of protein function. *Curr Mol Med.* 2004; 4: 529–38.
49. **Fuchs SM, Raines RT.** Polyarginine as a multifunctional fusion tag. *Protein Sci.* 2005; 14: 1538–44.
50. **Breitz HB, Weiden PL, Beaumier PL *et al.*** Clinical optimization of pretargeted radioimmunotherapy with antibody-streptavidin conjugate and 90Y-DOTA-biotin. *J Nucl Med.* 2000; 41: 131–40.
51. **Meyer DL, Schultz J, Lin Y *et al.*** Reduced antibody response to streptavidin through site-directed mutagenesis. *Protein Sci.* 2001; 10: 491–503.
52. **Skerra A.** Lipocalins as a scaffold. *Biochim Biophys Acta.* 2000; 1482: 337–50.
53. **Schlehuber S, Skerra A.** Anticalins as an alternative to antibody technology. *Expert Opin Biol Ther.* 2005; 5: 1453–62.